*Arab Journal of Nuclear Science and Applications, 48(4), (44-52) 2015*

# Physico-Chemical Properties of Carboxymethyl Cellulose (CMC)/ Nanosized Titanium Oxide ($TiO_2$) Gamma Irradiated Composite

**H.E. Ali, A. Atta* and M.M. Senna**
*Radiation chemistry department, National Center for Radiation Research and Technology (NCRRT),Nasr City, Cairo, Egypt*
**Radiation physics department, National Center for Radiation Research and Technology (NCRRT),Nasr City, Cairo, Egypt*

**Received: 11/12/2014** **Accepted: 26/1/2015**

## ABSTRACT

**In this work, $TiO_2$ nanoparticles were prepared by sol-gel method with or without a stabilizer as such as carboxy methylcellulose (CMC). $TiO_2$ nanoparticles was used to prepare CMC/$TiO_2$ composite. In addition, the prepared CMC/$TiO_2$ composites were irradiated by a dose from 10-30 kGy of gamma irradiation. The properties of the prepared CMC/$TiO_2$ composites were characterized by X-ray diffraction (XRD), transmutation electron microscopy (TEM), thermal gravimetric analysis TGA and UV. The obtained data indicated that the stabilizer (CMC) has a significant effect on the particle size distribution. Values of optical energy band gap $E_g$ decreased from 3 eV for CMC to 2.88 eV for CMC with $TiO_2$ whereas these values were decreased to 2.77 by gamma irradiation at a dose of 30 kGy. In addition, thermal gravimetric analysis (TGA) indicated that the thermal stability properties of CMC were increased by the addition of $TiO_2$ and gamma irradiation.**

***Key words: $TiO_2$, Carboxymethyl cellulose, gamma radiation, nanoparticles.***

## INTRODUCTION

Carboxymethyl cellulose (CMC) is an important industrial polymer with a wide range of applications in flocculation, drag reduction, detergents, textiles, paper, foods, drugs, and oil well drilling operation. CMC is a derivative of cellulose and formed by its reaction with sodium hydroxide and chloroacetic acid. It has a number of sodium carboxymethyl groups ($CH_2COONa$), introduced into the cellulose molecule, which promote water solubility. The various properties of CMC depend upon three factors: molecular weight of the polymer, average number of carboxyl content per anhydroglucose unit, and the distribution of carboxyl substituents along the polymer chains [1-3].

Nanotechnology is defined as the utilization of structures with at least one dimension of nanometer size for the construction of materials, devices or systems with novel or significantly improved properties due to their nano-size. Nanotechnology is an extremely powerful emerging technology that is expected to have a substantial impact on medical technology now and in the future. Nano-particles are commonly used in commercial products in the range of 1–100 nm [4].

$TiO_2$ is mainly applied as pigments, adsorbents, catalyst supports, filters, coatings, photoconductors, and dielectric materials. $TiO_2$ has been well known as a semiconductor with photocatalytic activities and has a great potential for applications such as environmental purification, decomposition of carbonic acid gas, and generation of hydrogen gas [5]. In addition, it had wide application due to its optical and electronic properties. It is used as an ingredient in sunscreen lotions and food products, as a pigment in paints and as semiconductors in the photocatalytic degradation of organic compounds [6]. In $TiO_2$, the crystalline phase, the composition and the surface states strongly affect the electronic structure and the charge properties [7] . The photocatalytic activity of $TiO_2$ depends on its resent phase. In most of these cases, the size of the $TiO_2$ particles is an important factor affecting

the performance of the materials. Therefore much research has been focused upon the reduction of the particle size.

There are three crystalline forms of $TiO_2$: anatase, rutile and brookite. Anatase phase is metastable and has the greater photocatalytic activity; rutile has a high chemical stability but is less active [8]. $TiO_2$ with a large quantity of anatase and a small quantity of rutile exhibits a higher photocatalitic activity than in the pure anatase or rutile phases [9]. The absorption spectrum of a semiconductor defines its possible uses. The useful semiconductors for photocatalysis have a band gap comparable to the energy of the photons of visible or ultraviolet light, having a value of $E_g < 3.5$ eV. The rutile has a direct band gap of 3.06 eV and an indirect band gap of 3.10 eV. On the other hand, the anatase has only an indirect band gap of 3.23 eV [10]. There have been reported values in the literature from 2.86 to 3.34 eV for the anatase phase, the differences being attributed to variations in the stoichiometric of the synthesis, the impurities content, the crystalline size and the type of electronic transition [11].

In this work, the physical properties are evaluated in the context of the band gap of the unirradiated and irradiated CMC with 10 % $TiO_2$, which expected to increase the absorbance of the longitude or the wave corresponding to the energy of the prohibited band by adding$TiO_2$ and gamma radiation exposure.

## EXPERIMENTAL

### 1. Preparation of TiO2 Nanoparticles

25 ml aliquot of titanium isopropoxide (95%, Alfa, Aesar, Germany) is added drop wise at room temperature, to 125 ml of 0.1 M nitric acid solution under vigorous stirring. A white precipitate is formed instantaneously. Immediately after the hydrolysis, the slurry is heated to 80 $^oC$ and stirred vigorously for 8 h in order to achieve the peptization (i.e., destruction of the agglomerates and dispersion into primary particles). A precipitate was obtained by centrifugation, where it was dried at 100 $^oC$ and calcined at 500 $^oC$ for 2h.

### 2. Preparation of CMC/$TiO_2$ Nanocomposites Films

5.0 gm of CMC (was a laboratory-grade chemical and purchased from El Gomhoria Company, Cairo, Egypt) was added to100 ml of distilled water with stirring for 4h until complete miscibility. During the stirring the required amount of $TiO_2$ (10%) was added to the solution. The mixture was removed, the foam was skimmed off and the solution was poured on leveled hydrophobic polystyrene petri dishes and dried for 48h at room temperature to form the desired films. The films were finally removed from the trays.

### Gamma Irradiation

Irradiation was carried out in the cobalt-60 gamma cell, (made in Russia) at a dose rate of 4.8 $kGyh^{-1}$ in air, at National Center for Radiation Research and Technology (NCRRT).

### Measurements and Analysis

The structure of CMC polymer and CMC/TiO2 nanocomposites films were carried out by a fully computerized X-ray diffractometer (Shimadzu type XD-DI). The surface morphology and the particle size were investigated by Transmission electron microscope; model JEM100CS, Jeol Electron Microscope, Japan, working at an acceleration voltage of 80 kV. The optical absorbance measurements of the prepared samples were carried out at room temperature using a double beam Shimadzu UV-VIS spectrophotometer in the wavelength range 200-1100 nm. The thermal behavior was investigated using thermogravimetric analysis, shimadzu-50 (TGA-50) at a heating rate of 10 $^oC$/min., and differential Scanning Calorimetry shimadzu (DSC-50), Japan. The thermal measurements

were carried out with heating rate of 10 °C/min., and under flowing nitrogen atmosphere at a rate of 20 ml/min.

## RESULTS AND DISCUSSION

### 1. X-RAY DIFFRACTION

XRD patterns of CMC/$TiO_2$ (10%) nanoparticles are shown in Fig.1. The XRD patterns exhibited strong diffraction peaks at 25° and 48° indicating $TiO_2$ in the anatase phase .On the other hand diffraction peaks at 27°, 36° and 55° indicating $TiO_2$ in the rutile phase. As can be seen, the anatase phase is the dominant phase observed in figure 1. The peak intensity of the $TiO_2$ decreases with increasing gamma radiation and the XRD of CMC polymer is amorphous.

### 2. TRANSMISSION ELECTRON MICROSCOPY (TEM)

TEM bright field images of $TiO_2$ nano powders are shown in Fig. 2, from which, it is clear that the particle size of samples are nanoscale with the grain size about 10-17 nm, the results which are in close agreement with XRD results.
Scherrer equation relates the FWHM (b), in radians, of a XRD peak to the crystallite size (L) as the following [12].

$$L = K\lambda / b \cos \theta \qquad (1)$$

Where λ is the wavelength of the X-ray beam (λ = 0.15425 nm of CuKα1), θ is the corresponding Bragg angle and K is Scherrer constant. The crystallite sizes, corresponding to the most intense peak of the pristine and irradiated films, were calculated as illustrated in Table 1.

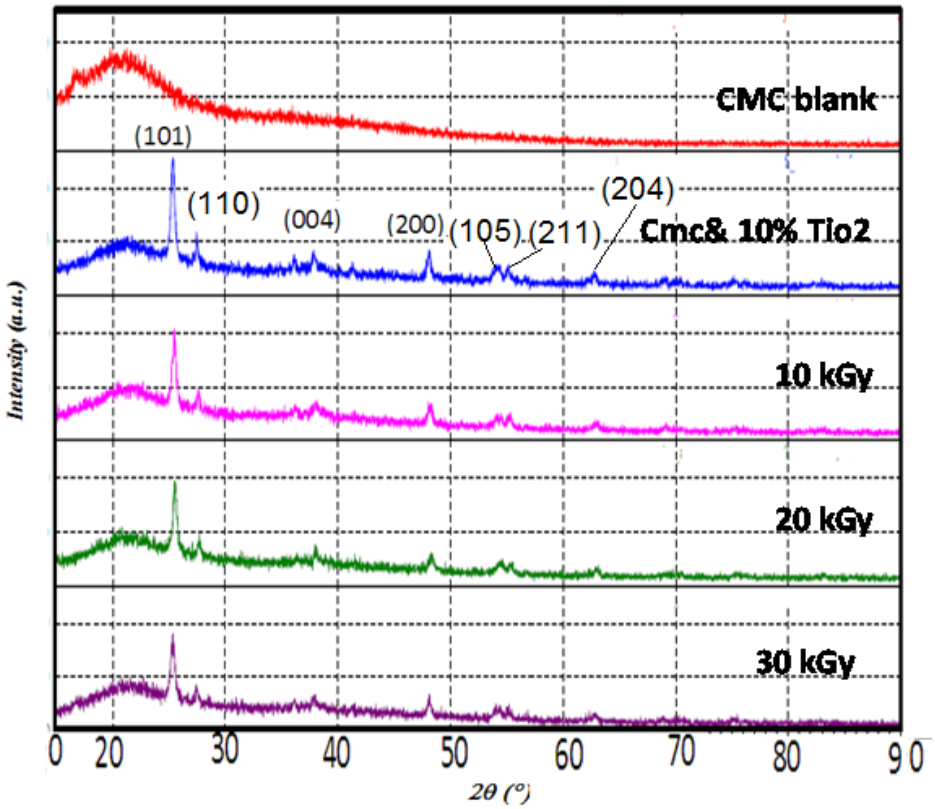


**Fig. (1):** XRD for the CMC, CMC/10%$TiO_2$ and irradiated CMC/$TiO_2$(10%).

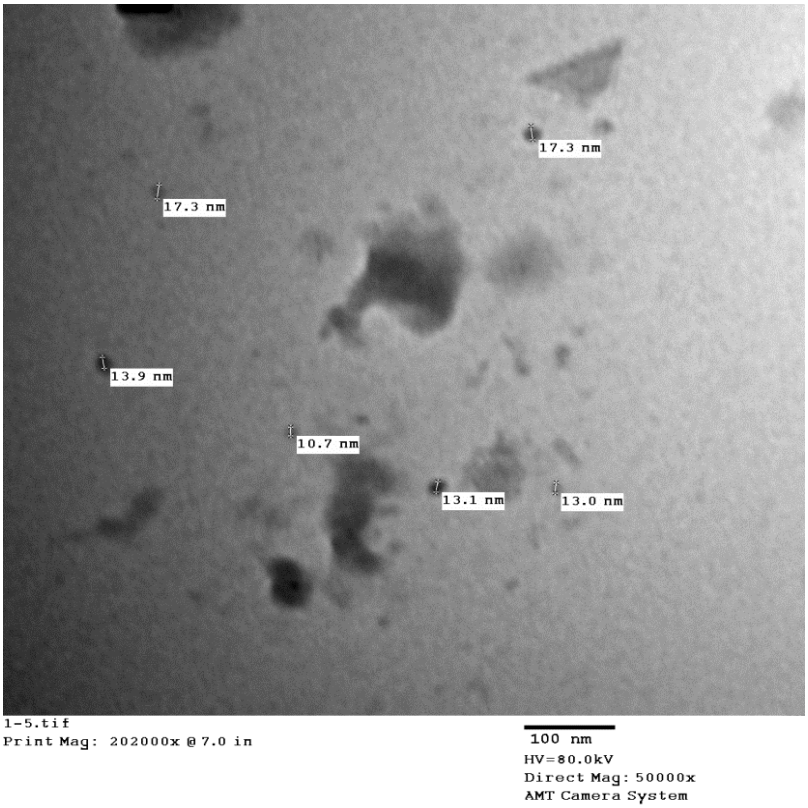


**Fig. (2):** TEM micrograph of $TiO_2$.

**Table (1):** Intense peaks (2θ), FWHM and the crystallite size (L) for the blank and irradiated $TiO_2$ doped CMC films.

| | 2 θ | FWHM (Radian) | d ($A^0$) | Crystallite size (nm) | Average crystallite size (nm) |
|---|---|---|---|---|---|
| CMC/10%$TiO_2$ | 25.30 | 0.007330 | 3.50 | 21.56605 | 24.34261 |
| | 48.10 | 0.006632 | 1.89 | 25.46848 | |
| | 27.45 | 0.006109 | 3.24 | 25.99329 | |
| 10kGy | 25.40 | 0.007505 | 3.49 | 21.06865 | 22.46376 |
| | 48.15 | 0.008029 | 1.88 | 21.04328 | |
| | 27.60 | 0.006283 | 3.23 | 25.27936 | |
| 20 kGy | 25.50 | 0.007679 | 3.48 | 20.59387 | 21.51105 |
| | 48.24 | 0.009425 | 1.88 | 17.93205 | |
| | 27.70 | 0.006109 | 3.22 | 26.00721 | |
| 30 kGy | 25.30 | 0.008203 | 3.51 | 19.27179 | 19.31667 |
| | 48.10 | 0.006632 | 1.89 | 25.46848 | |
| | 27.60 | 0.011868 | 4.30 | 13.20975 | |

## 3. Optical Properties

The absorbance spectra for CMC blank, CMC/10%$TiO_2$ and irradiated CMC/10%$TiO_2$ (10, 20, 30 kGy) are shown in Fig 3. It is observed that the same behavior happened for the irradiated sample, but the value of absorption for the irradiation samples increases slightly than unirradiated

samples. This behavior is attributed to the increase in the energy of atoms that leads to the increase of the number of collision between incident atoms , which in turn , leads to the decreasing the transmittance and increasing absorption as shown in Fig 3. This behavior shows clearly the enhancement of absorption properties after addition of $TiO_2$. The doped $TiO_2$ appear to be more stable under UV irradiation compared with the non doped ones.
The optical absorption edge was analyzed by the following relation [13,14].

$$\alpha = A(h\nu - E_g)^r \qquad (2)$$

Where A is the constant, h is the Plank's constant, ν is the frequency of the radiation, and $E_g$ is the optical energy gap. The type of transition is responsible for the optical absorption that depends on the value of r, where r represents an index that can take any of the values 1/2, 3/2, 2 or 3. x = 1/2 for the direct transition (in case CMC& 10%$Tio_2$) and x = 2 for the indirect transition (in case of CMC polymer). The energy gap was shown in fig (4a) for CMC polymer, where the energy gab for CMC/10%$TiO_2$ after and before irradiation is shown in Fig. 4b.

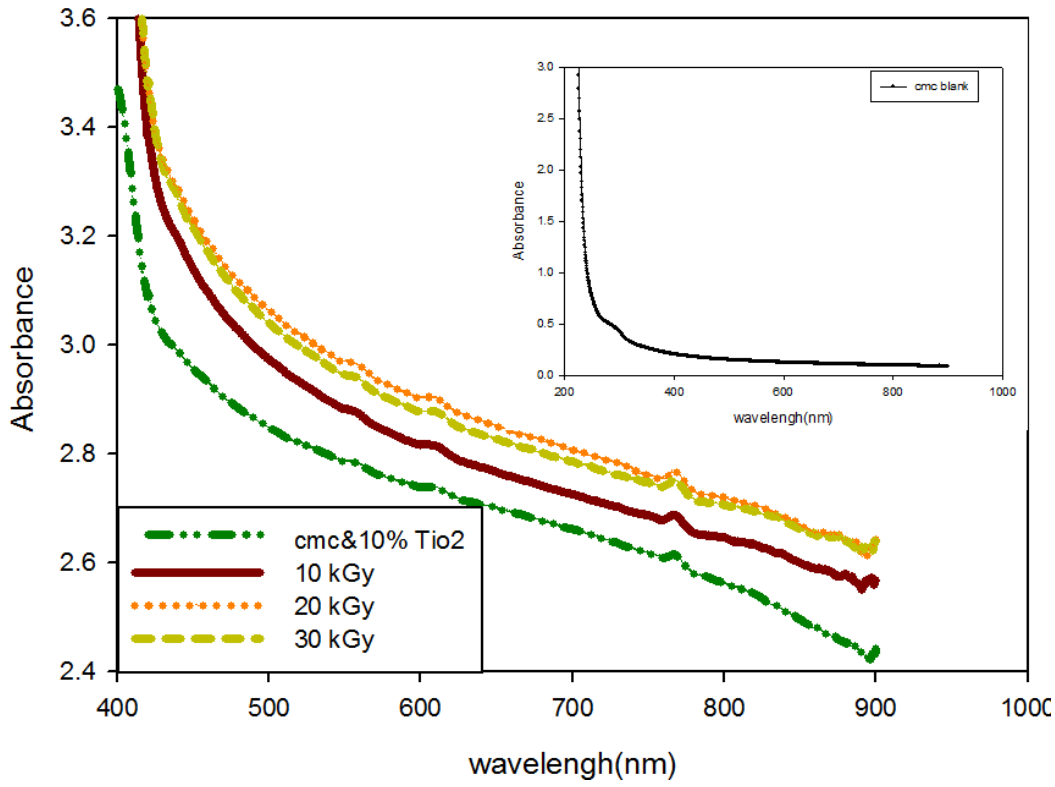


**Fig. (3):** Absorbance spectra of the CMC, CMC/10%$TiO_2$ and irradiated CMC/10%$TiO_2$

Results of the optical energy gap $E_g$ measurements for blank, CMC/10%$TiO_2$and irradiated CMC/10%$TiO_2$ are shown in Table (2). The results clearly show that the values of optical energy band gap $E_g$ decreases from 3 eV for CMC to 2.88 eV for CMC/10% $TiO_2$ . $TiO_2$ doping causes decreasing in band gap energy, which is the minimum energy to promote the excited electron from valence band to conduction band. A similar trend was also observed in Lan Sun et al. (2009) [15] and He et al. (2002) [16]. Both studies concluded that the absorption edge shift possibly linked to the interaction of metal and $TiO_2$. This result corresponded to wavelength absorption analysis. Not only by reducing band gap energy, but the $TiO_2$ dopant was also able to prevent charge recombination between electron–hole

pairs. Thus, the photocatalytic reactivity's efficiency improved. It was found that the value of optical energy band gap decreases from 2.88 eV for unirradiated CMC / $TiO_2$ sample to 2.77 eV for the irradiated sample with 30 kGy . The value of the direct allowed band gap was decreased with respect to the band gap of unirradiated samples. It is well known that the exposure of solid materials to gamma rays induce structured defects known as color centers or oxygen vacancies in oxides.

The increase of the free radicals, due to gamma radiation, may increase the mobility of the carriers. Which causes the reduction of the energy required for transitions, i.e. reduction in the optical energy gap.

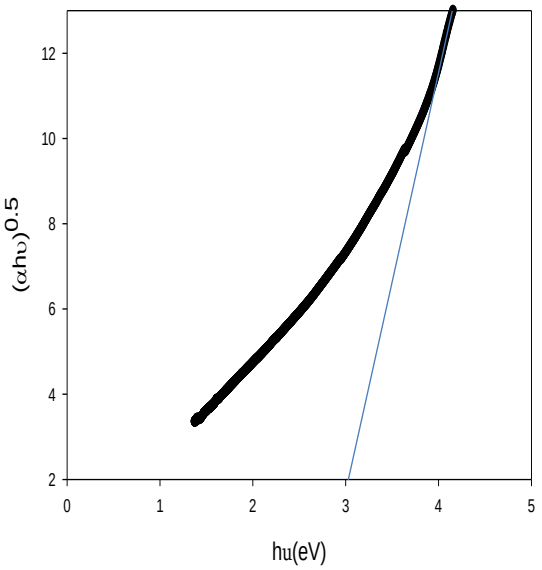


**Fig. (4a) :** Energy band gap spectra for CMC blank

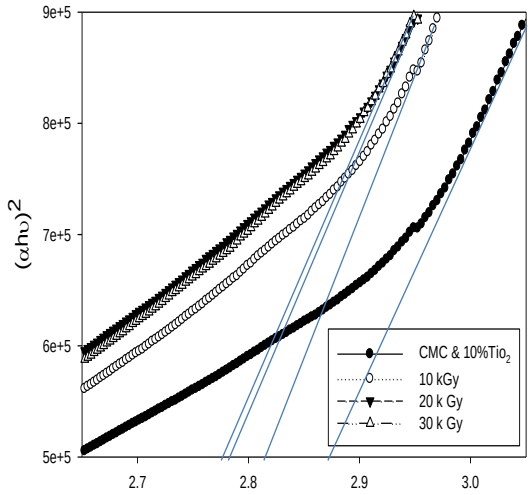


**Fig. (4b):** Energy band gap spectra for of CMC/10%$TiO_2$ exposed to various doses of gamma irradiation

**Table (2):** Values of $E_g$ for the unirradiated and irradiated CMC/10%$TiO_2$ nanocomposites.

| Sample types | $E_g$ (ev) |
|---|---|
| CMC | 3. 00 |
| CMC/10%$TiO_2$ | 2.88 |
| CMC/10%$TiO_2$ (10kgy) | 2.82 |
| CMC/10%$TiO_2$ (20kgy) | 2.78 |
| CMC/10%$TiO_2$ (30 kgy) | 2.77 |

## 4. Thermogravimetric Analysis (TGA)

Thermogravimetric analysis (TGA) has been the conventional and most popular technique used to study the thermal stability and decomposition of polymers [17-18]. TGA was used to investigate experimentally the thermal stability of the polymer with $TiO_2$. Fig. 5 shows TGA and the rate of thermal decomposition of CMC blank and CMC/$TiO_2$ composites at 10% of $TiO_2$ nanoparticles at different doses of gamma radiation. In the case of CMC two distinct zones are observed where the weight is being lost. The initial weight loss is due to the presence of small amount of moisture in the sample. The second loss is due to the loss of $CO_2$ from the polysaccharide. As there are $COO^{2-}$ group in the case of CMC, it is decarboxylated in this temperature range.

Over all the decomposition temperature ranges up to 500 °C, the thermal stability was found to increase with increasing $TiO_2$ nanoparticles. On the other hand the effect of radiation on the thermal properties of CMC/$TiO_2$ 10% composites. It is found that the thermal stability increased with increasing the irradiation dose up to (10 kGy). Then the thermal stability decreased by increasing gamma irradiation dose. But still more than CMC blank that's may be due to degradation which result from irradiation. It can be noticed that the initial water content does not affect the onset of decomposition temperature, because all water evaporates from the sample prior to reaching the decomposition temperature. Dehydration and decomposition have generally been considered as two separated processes associated with the degradation mechanisms of CMC in the open system.

**5. Diffraction Scanning Calomitry (DSC)**

Diffraction Scanning Calomitry **(**DSC) curves were plotted for CMC and the CMC containing constant ratio of 10% of $TiO_2$ nanoparticles, before and after gamma irradiation to different doses as shown in Fig 6. CMC shows a distinct feature in the DSC curve having one endotherm (76 °C) and others at relatively higher temperatures due to the decomposition of the main chain. This step is followed by depolymerisation, which proceeds due to the cleavage of glycosidic linkages. The other small exothermic peaks at about 280 °C and above are due to the combustion of the degraded products.

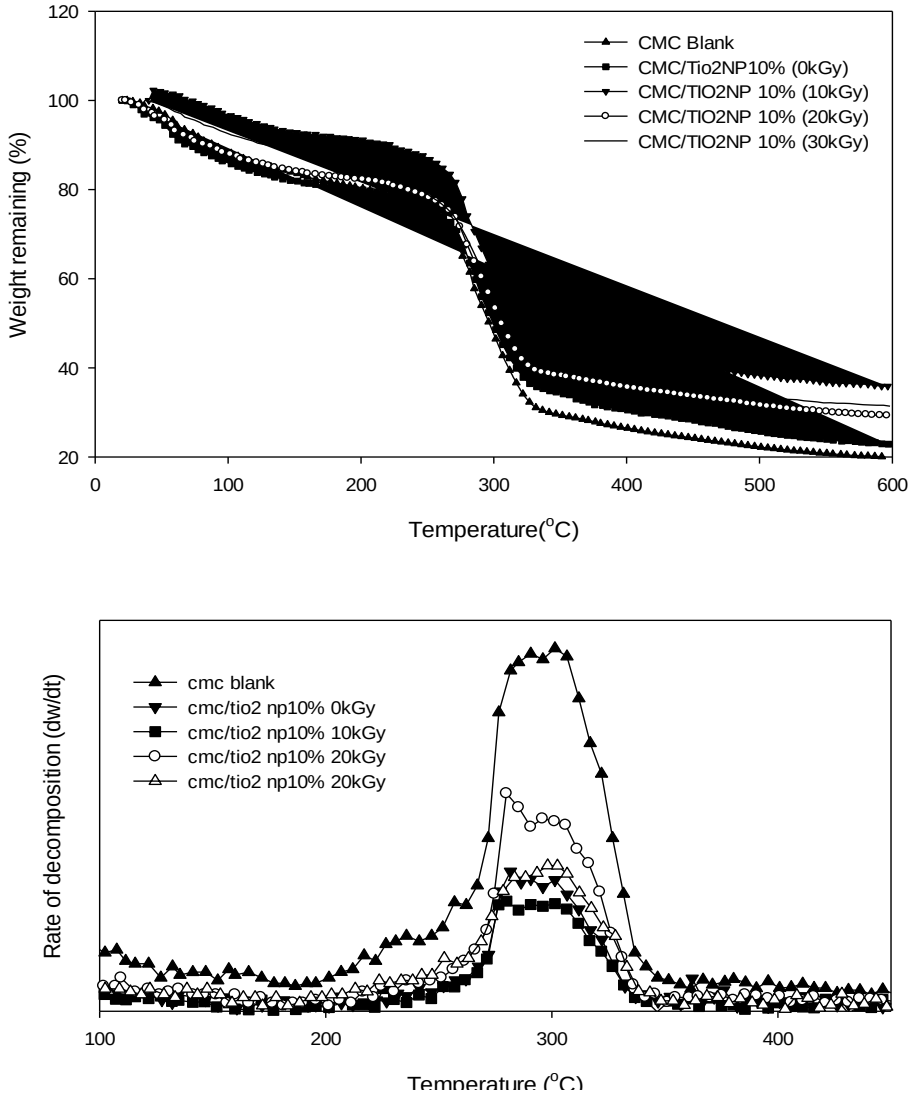


**Fig. (5):** TGA thermograms and the rate of thermal decomposition reaction of unirradiated CMC/10%$TiO_2$ and that exposed to various doses of gamma radiation.

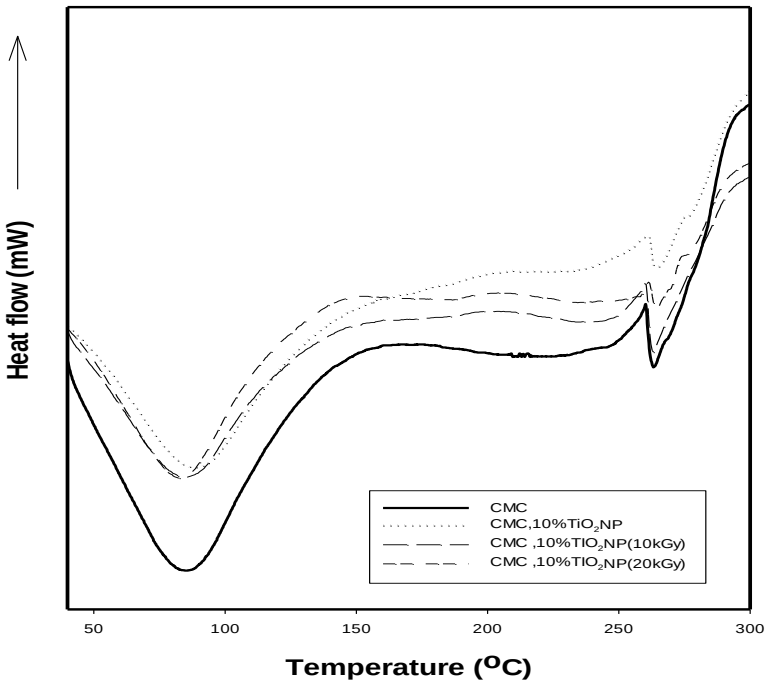


**Fig. (6):** DSC Thermograms of CMC/10%$TiO_2$ exposed to various doses of gamma radiation.

## CONCLUSIONS

CMC/$TiO_2$ nanocomposites have been prepared by the sol–gel method. The XRD results exhibits that the samples anatase phase has been observed as the dominant phase, and indicated also the presence of the rutile phase. The TEM images indicated the particles are in nanoscale size and the XRD diffraction pattern peak intensity of the $TiO_2$ decreases with increasing gamma radiation. The $TiO_2$ enhances the thermal stability of the CMC.

## REFERENCES

(1) A. Baar, and W.M. Kulicke, Macromolecular Cellular Physics, 195(1994) 1483–1492.

(2) K. Kamide, K. Okajima, K. Kowsaka, K.T. Matsui, S. Nomuraand, K. Hikichi, Polymer J., 17 (1985) 909–918.

(3) J. Reuben and H. T. Conner, Carbohydrate research. 115(1983)1–13.

(4) E. Russell, Textile Horizons, 9 (2002) 7–9.

(5) Q. Zhang, L. Gao and J. Guo, J. Eur. Ceram. Soc. 20(2000) 2153-2158.

(6) K. Reddy, S. Manorama, A. Redd, Mater Chem. Phys; 78(2002)239-245.

(7) L. Jing, S. Li , S. Song, L. Xue, H. Fu, Solar Energy Mater Solar Cells; 92(2008)1030.

(8) G. Wang, J. Mol Catal A: Chem 274(2007)185-91.

(9) S. Sahni, B. Reddy , B. Murty , Mater Sci Eng A 452-453 (2007) 758-62.

(10) A. Welte, C. Waldauf, C. Brabec, P. Wellmann, Thin Solid Films, 516 (2008)7256-9.

(11) F. Hossain, L. Sheppard, J. Nowotny, G. Murch, J Phys Chem Solids 69 (2008) 1820-8.

(12) M. M. El-Nahass, A.M. Farag, K.F. Abd El-Rahman and A.A. Darwish, Laser Technol.Opt. 37(2005) 513.

(13) A. L. Fahrenbruch and R. H. Bude, Fundamentals of Solar Cells (1983) (New York: Academic) 49

(14) B. Pejova, A. Tevski and I. Grozdanov, J. Solid State Chem. 17(2004), 4785.

(15) L. Sun .J. Li, C. Wang, S. Li,Y. Lai,H. Chen, C. Lin, Ultrasound aided photochemical synthesis of Ag loaded TiO2 nanotube arrays to enhance photocatalytic activity, Journal of Hazardous Materials, 171 (2009) 1045-1050

(16) J. He , I. Ichinose, T. Kunitake, A. Nakao, In situ synthesis of nobel metal nanoparticles in ultrathin TiO2 – gel films by a combination of ion-exchange and reduction processes, Langmuir 18 (2002) 10005-10010.

(17) M. Magdy Senna, M. Rasha Mohamed, N. Amira Shehab-Eldin, S. Sabrnal El-Hamouly ,) J.of Indust. and Eng.g Chem. 18, (2012)1654–1661.

(18) M. Magdy Senna ,K. Yasser Abdel-Moneam, A. Osama Gamal, A. Abdallah Alarifi,

J. of Ind. and Eng. Chem. 19, (2013) 48–55

(19) L. Guinesi. A. da Roz,E. Corradini, L. Mattoso, E. Teixeira , A. Curvelo . Thermochim Acta, 447, (2006),190–5.

(20) P. Aggarwal, D. Dollimore , Talanta ,43.(1996)1527–32.